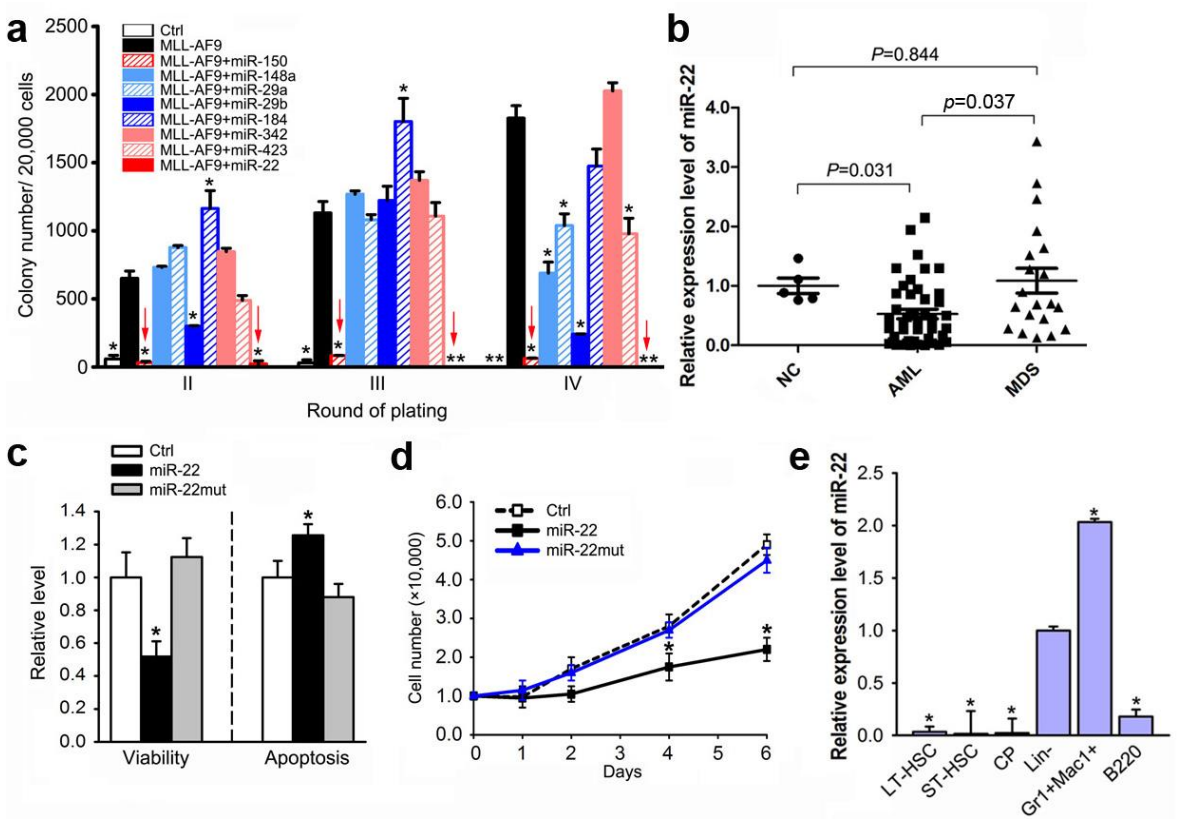


**Supplementary Figure 1.** miR-22, which is down-regulated in AML, inhibits AML cell transformation and growth. (**a**) Comparison of effects of a set of miRNAs, which are down-regulated in AML, on *MLL-AF9*-induced colony forming. Colony-forming/replating assays (CFAs) were performed using mouse BM progenitor (lineage negative; $Lin^-$) cells transduced with retrovirus of MSCV-neo+MSCV-PIG (Ctrl), MSCV-neo-*MLL-AF9*+MSCV-PIG (MLL-AF9), or MSCV-neo-*MLL-AF9*+MSCV-PIG-miR-150/miR-148a/miR-29a/miR-29b/miR-184/miR-342/miR-423/miR-22. (**b**) qPCR confirmation of the down-regulation of miR-22 in AML. Expression level of miR-22 in the mononuclear cells of 5 normal MNC control (NC), 42 AML (including 17 *MLL*-rearranged AML, 13 t(8;21), 5 t(15;17) and 7 inv(16)) and 20 MDS (including 17 (+8) and 3 (-7)) samples are shown. (**c, d**) Effects of miR-22 on the viability and apoptosis (**c**) as well as growth (**d**) of AML cells. MONOMAC-6 cells were transfected with MSCV-PIG (Ctrl), MSCV-PIG-miR-22 (miR-22), or miR-22 mutant (miR-22mut) plasmids. Cell viability and apoptosis were detected 48 hrs post-transfection. Cell growth was assessed by cell counts at a series of time points post-transfection. (**e**) Expression levels of miR-22 in various sub-populations of mouse normal hematopoietic cells. Expression levels of miR-22 in long-term HSC (LT-HSC; $Lin^-Sca1^+c\text{-}Kit^+Flk2^-$, $LSKF^-$), short-term HSC (ST-HSC; $Lin^-Sca1^+c\text{-}Kit^+Flk2^+$, $LSKF^+$), committed progenitor (CP; $Lin^-Sca1^-c\text{-}Kit^+$), $Gr\text{-}1^+/Mac\text{-}1^+$ myeloid and $B220^+$ lymphoid cells, were normalized to the level in lineage negative ($Lin^-$) cells. Mean±SD values are shown. *, $p<0.05$. All the $p$ values shown in this figure were generated by $t$-test.

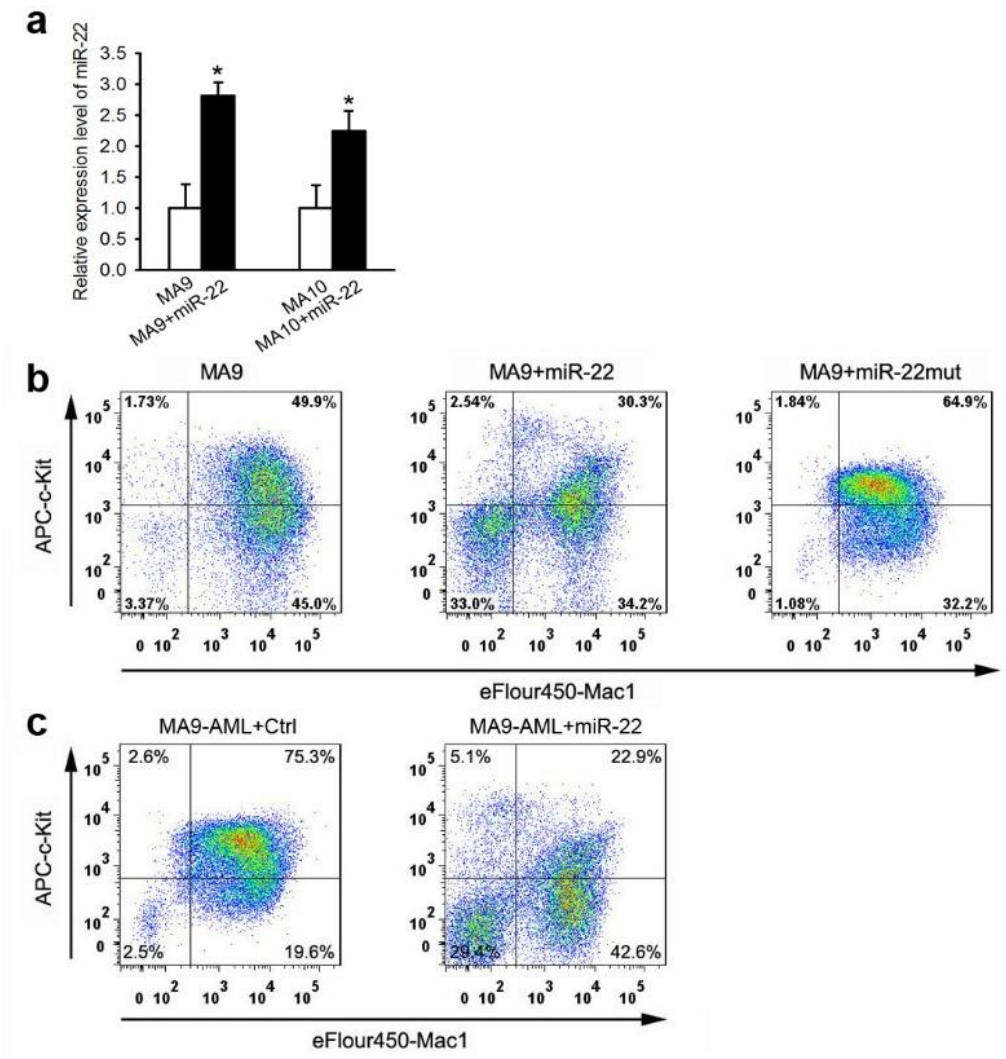


**Supplementary Figure 2.** Role of miR-22 in AML *in vivo*. (**a**) Overexpression level of miR-22 in bone marrow cells of MLL-AF9 and MLL-AF10-induced primary leukemic mice. 3~5 independent leukemic mice are included in each group. Mean±SD values are shown. *, $p<0.05$, *t*-test. (**b, c**) Flow cytometry analyses of the BM cells of both primary bone marrow transplantation (BMT) recipient mice (**b**) or secondary BMT recipient mice (**c**). 0.5 million mouse BM cells collected at the end point were stained with APC-conjugated anti-mouse c-Kit or eFluor®450-conjugated anti-mouse CD11b (Mac-1) antibodies. Proportions of c-Kit$^+$ and/or Mac1$^+$ cells are shown.

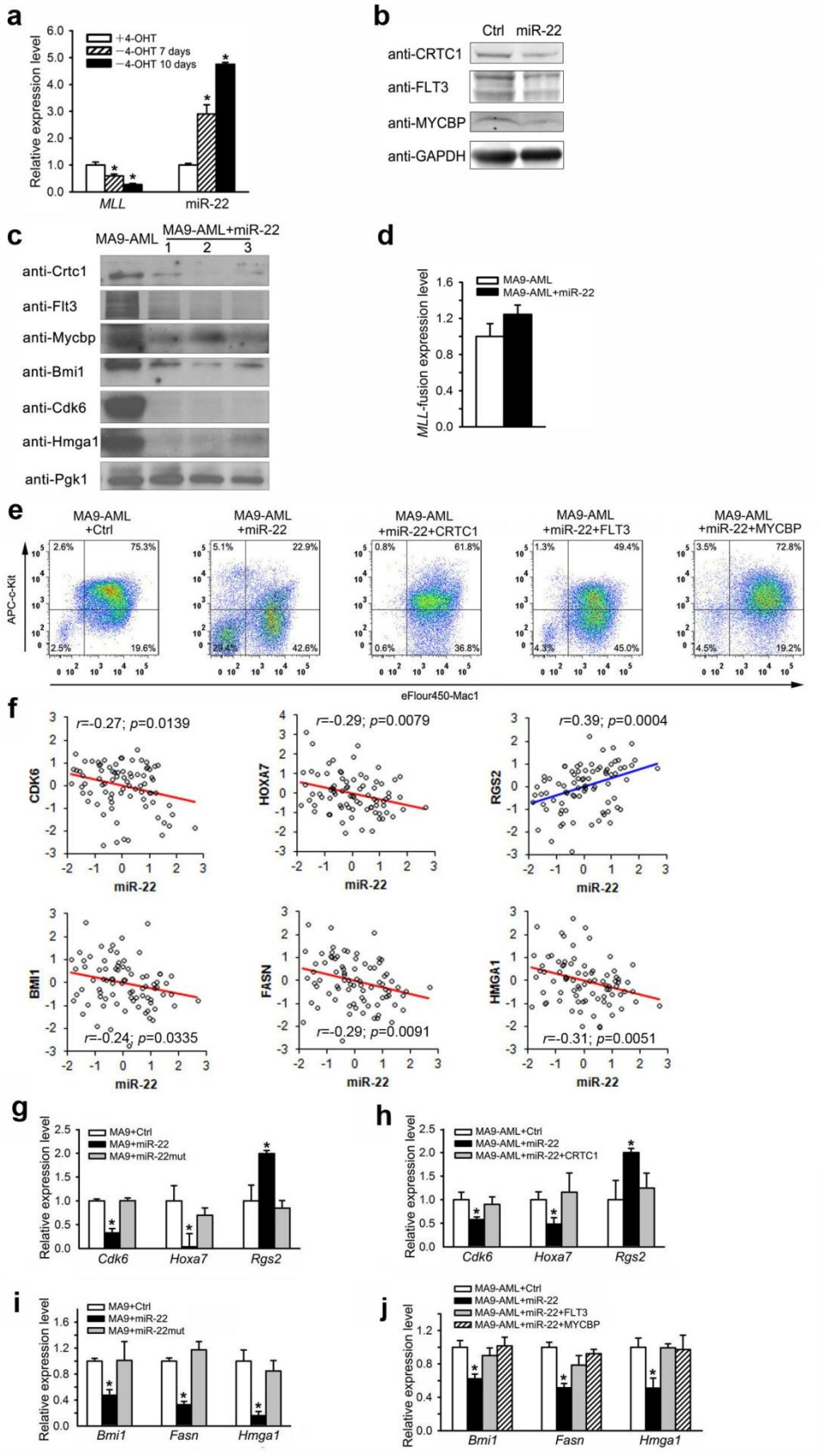
a
Relative expression level
+4-OHT
−4-OHT 7 days
−4-OHT 10 days
MLL
miR-22
b
Ctrl
miR-22
anti-CRTC1
anti-FLT3
anti-MYCBP
anti-GAPDH
c
MA9-AML
MA9-AML+miR-22
1
2
3
anti-Crtc1
anti-Flt3
anti-Mycbp
anti-Bmi1
anti-Cdk6
anti-Hmga1
anti-Pgk1
d
MA9-AML
MA9-AML+miR-22
MLL-fusion expression level
e
MA9-AML +Ctrl
MA9-AML +miR-22
MA9-AML +miR-22+CRTC1
MA9-AML +miR-22+FLT3
MA9-AML +miR-22+MYCBP
APC-c-Kit
eFlour450-Mac1
2.6%
75.3%
2.5%
19.6%
5.1%
22.9%
28.4%
42.6%
0.8%
61.8%
0.6%
36.8%
1.3%
49.4%
4.3%
45.0%
3.5%
72.8%
4.5%
19.2%
f
CDK6
r=-0.27; p=0.0139
HOXA7
r=-0.29; p=0.0079
RGS2
r=0.39; p=0.0004
BMI1
r=-0.24; p=0.0335
FASN
r=-0.29; p=0.0091
HMGA1
r=-0.31; p=0.0051
miR-22
g
MA9+Ctrl
MA9+miR-22
MA9+miR-22mut
Relative expression level
Cdk6
Hoxa7
Rgs2
h
MA9-AML+Ctrl
MA9-AML+miR-22
MA9-AML+miR-22+CRTC1
Relative expression level
Cdk6
Hoxa7
Rgs2
i
MA9+Ctrl
MA9+miR-22
MA9+miR-22mut
Relative expression level
Bmi1
Fasn
Hmga1
j
MA9-AML+Ctrl
MA9-AML+miR-22
MA9-AML+miR-22+FLT3
MA9-AML+miR-22+MYCBP
Relative expression level
Bmi1
Fasn
Hmga1

**Supplementary Figure 3.** Repression of the CREB and MYC pathways by miR-22. (**a**) Up-regulation of miR-22 level in *MLL-ENL*-ERtm cells after withdrawal of 4-OHT for 0, 7 or 10 days. (**b**) Down-regulation of CRTC1, FLT3 and MYCBP at the protein level by miR-22. MONOMAC-6 cells were transfected with MSCV-PIG-miR-22 (miR-22) or MSCV-PIG vector (Ctrl). Protein extractions of the cells were analyzed through Western-blotting assays 48 hrs post-transfection. (**c**) Down-regulation of Crtc1, Flt3, Mycbp, Bmi1, Cdk6 and Hmga1 by miR-22 overexpression. Protein levels in BM blast cells of leukemic mice transplanted with *MLL-AF9* or *MLL-AF9*+miR-22 primary leukemic cells are shown. (**d**) miR-22 overexpression showed no significant influence on the level of *MLL*-fusion in *MLL-AF9*-leukemic mouse BM cells. Mouse BM progenitor cells bearing MLL-AF9 were retrovirally transduced with MSCV-PIG-miR-22 or MSCV-PIG vector. After 7 days' selection with puromycin, *MLL* levels were detected through qPCR. (**e**) Flow cytometry analyses of the BM cells of secondary BMT mice**.** 0.5 million mouse BM cells collected at the end point were stained with APC-conjugated anti-mouse c-Kit or eFluor®450-conjugated anti-mouse CD11b (Mac-1) antibodies. Proportions of c-Kit$^+$ and/or Mac1$^+$ cells are shown. (**f**) Correlation between the expression levels of miR-22 and *CDK6*, *HOXA7*, *RGS2*, *BMI1*, *FASN* or *HMGA1* in In-house_81S. The correlation coefficient (*r*) and *p* values were detected by "Pearson Correlation", and the correlation regression lines were drawn with the "linear regression" algorithm. (**g-j**) Expression levels of the CREB downstream genes *Cdk6, Hoxa7* and *Rgs2*, as well as the MYC downstream genes *Bmi1, Fasn* and *Hmga1* were detected in the BM cells of the primary BMT recipient mice (**g, i**) or the secondary BMT recipients (**h, j**). The primary transplanted mice include *MLL-AF9*+Ctrl, *MLL-AF9*+miR-22, and *MLL-AF9*+miR-22 mutant (miR-22mut). The secondary recipients were transplanted with the blast cells of the primary *MLL-AF9* mice retrovirally transduced with MSCVneo+MSCV-PIG (MA9-AML+Ctrl), MSCVneo-miR-22+MSCV-PIG (MA9-AML+miR-22), or MSCVneo-miR-22+MSCV-PIG-*CRTC1/FLT3/MYCBP* (MA9-AML+miR-22+CRTC1/FLT3/MYCBP). n=5 for each group. Mean±SD values of three replicates are shown. *, $p<0.05$. All the *p* values shown in this figure were generated by *t*-test, except for those shown in Figure 3F that were generated by Pearson correlation test.

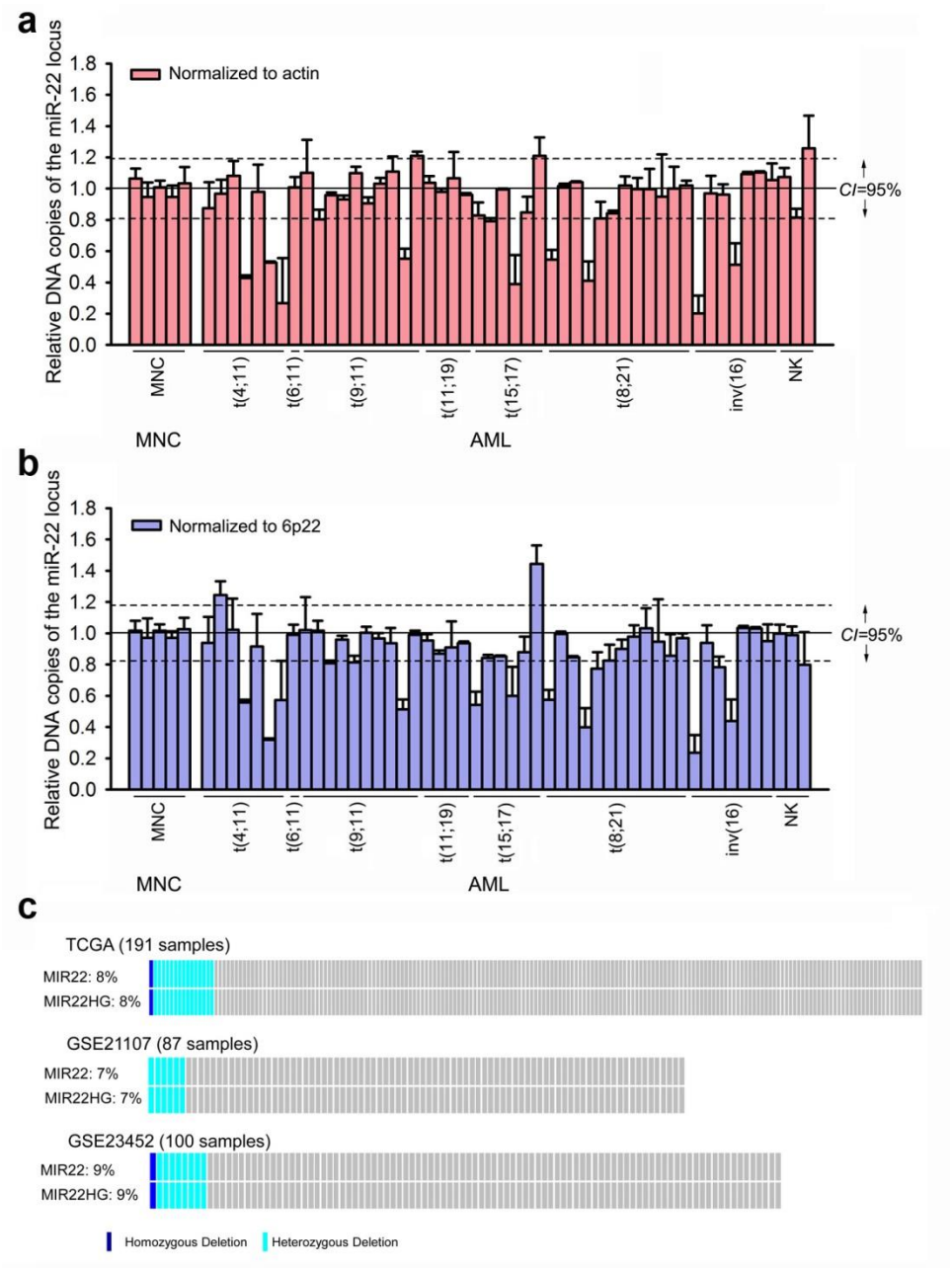


**Supplementary Figure 4.** DNA copy-number loss of the miR-22 gene locus in AML. (**a, b**) DNA copy number of the miR-22 gene locus of 50 AML samples and 5 normal controls were tested. qPCR data were normalized against the chromosomal region of *actin* (**a**) or *6p22* (**b**) probe. Mean values, standard deviations (error bars), and the 95% confidence internal (*CI*) are shown. (**c**) DNA copy-number loss of miR-22 in three independent AML datasets are shown. *Dark blue*: Homozygous deletion; *Cyan*: Heterozygous deletion.

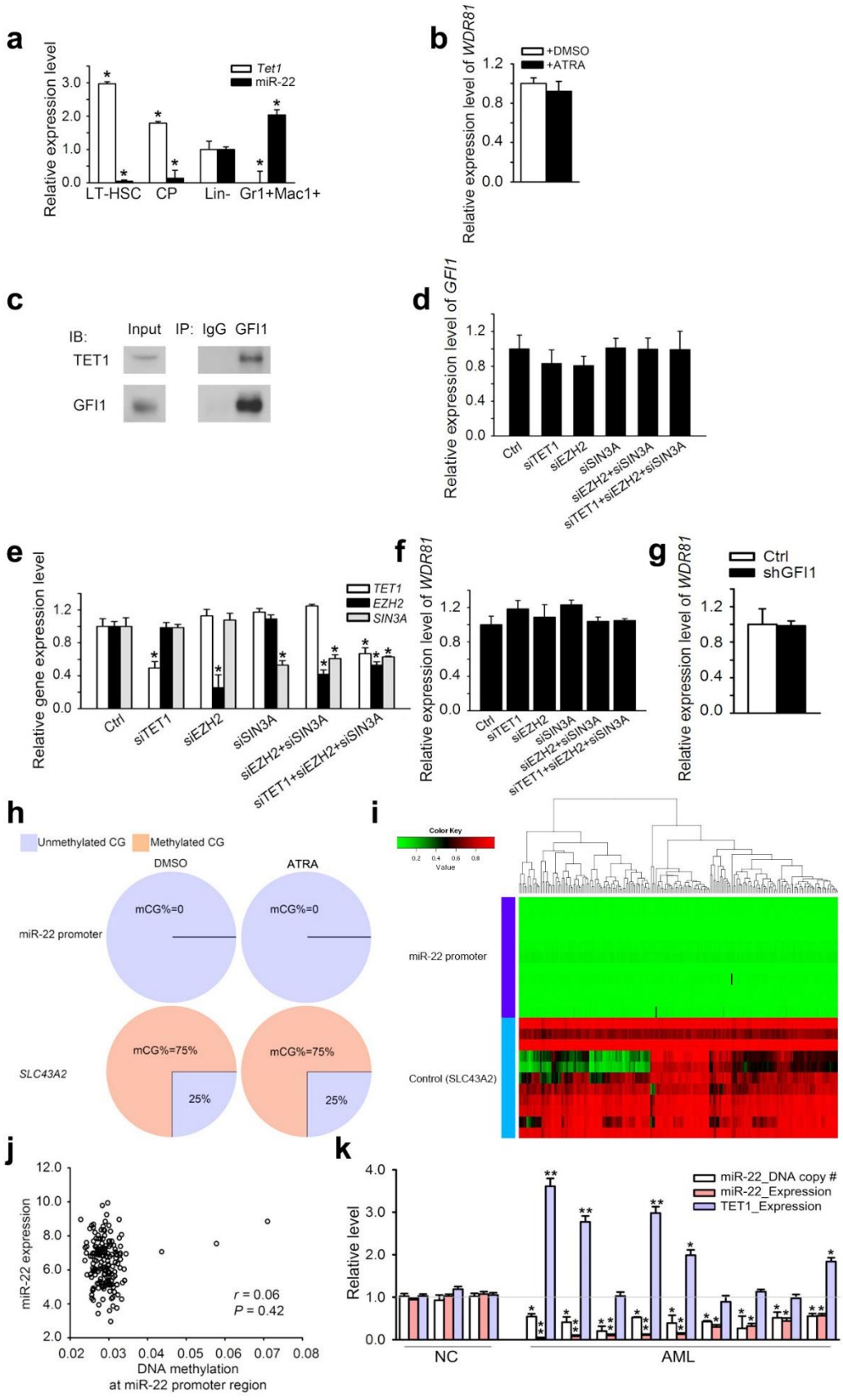
a
Relative expression level
Tet1
miR-22
LT-HSC
CP
Lin-
Gr1+Mac1+
b
Relative expression level of WDR81
+DMSO
+ATRA
c
IB:
Input
IP: IgG
GFI1
TET1
GFI1
d
Relative expression level of GFI1
Ctrl
siTET1
siEZH2
siSIN3A
siEZH2+siSIN3A
siTET1+siEZH2+siSIN3A
e
Relative gene expression level
TET1
EZH2
SIN3A
f
Relative expression level of WDR81
g
Relative expression level of WDR81
Ctrl
shGFI1
h
Unmethylated CG
Methylated CG
DMSO
ATRA
miR-22 promoter
SLC43A2
mCG%=0
mCG%=75%
25%
i
Color Key
Value
miR-22 promoter
Control (SLC43A2)
j
miR-22 expression
r = 0.06
P = 0.42
DNA methylation
at miR-22 promoter region
k
Relative level
miR-22_DNA copy #
miR-22_Expression
TET1_Expression
NC
AML

**Supplementary Figure 5.** Involvement of TET1 in miR-22 regulation. (**a**) Expression levels of Tet1 and miR-22 in various sub-populations of mouse normal hematopoietic cells. Gene expression levels in long-term HSC (LT-HSC; $Lin^{-}Sca1^{+}c\text{-}Kit^{+}Flk2^{-}$, $LSKF^{-}$), committed progenitor (CP; $Lin^{-}Sca1^{-}c\text{-}Kit^{+}$) and $Gr\text{-}1^{+}/Mac\text{-}1^{+}$ myeloid cells, were normalized to the level in lineage negative ($Lin^{-}$) cells. (**b**) Expression of *WDR81* in THP-1 cells 72 hours post-treatment with 1 μM ATRA or DMSO control. (**c**) Co-immunoprecipitation showing the binding between GFI1 and TET1 in HEK293T cells. (**d**) Effects of knockdown of *TET1*, *EZH2* and/or *SIN3A* on *GFI1* expression. (**e**) siRNA knockdown effects on *TET1, EZH2* and *SIN3A* in THP-1 cells. Gene levels were detected 48 hrs post-transfection. (**f**) Effects of knockdown of *TET1*, *EZH2* and/or *SIN3A* on *WDR81* expression. The expression level of *WDR81*was detected in THP-1 cells 72 hours post-transfection with siRNAs targeting *TET1, EZH2* and/or *SIN3A*. (**g**) Effects of knockdown of *GFI1* on *WDR81* expression. The expression level of *WDR81* was detected in THP-1 cells transduced with lentiviral vectored *GFI1* shRNA or control shRNA. (**h**) DNA methylation at miR-22 promoter region determined by bisulfite sequencing. Percentage of methylated CG (mCG%) at miR-22 promoter region in THP-1 cells treated with DMSO or 1 μM ATRA for 72 hrs were analyzed, with *SLC43A2* (100 kbps downstream of miR-22 promoter) as a positive control of DNA methylation. (**i**) DNA methylation level at miR-22 promoter region of 194 AML patient samples from TCGA_194S is shown, with *SLC43A2* as a positive control of DNA methylation. (**j**) Correlation analysis between miR-22 methylation and expression in 170 AML patient samples with both methylation and gene expression data from TCGA_194S. (**k**) qPCR analysis of miR-22 and *TET1* expression in AML samples with DNA copy-number loss of miR-22. A total of 9 AML and 3 normal controls samples, all been studied in the analyses of Supplementary Figure 4a/b, are included. The expression levels of miR-22 and TET1 are normalized to *RNU48* and *actin*, respectively. The DNA copy numbers are normalized to those at the gene locus of *actin*. Mean±SD values are shown. *, $p<0.05$; **, $p<0.01$. All the *p* values shown in this figure were generated by *t*-test, except for the one shown in Figure 5J that was generated by Pearson correlation test.

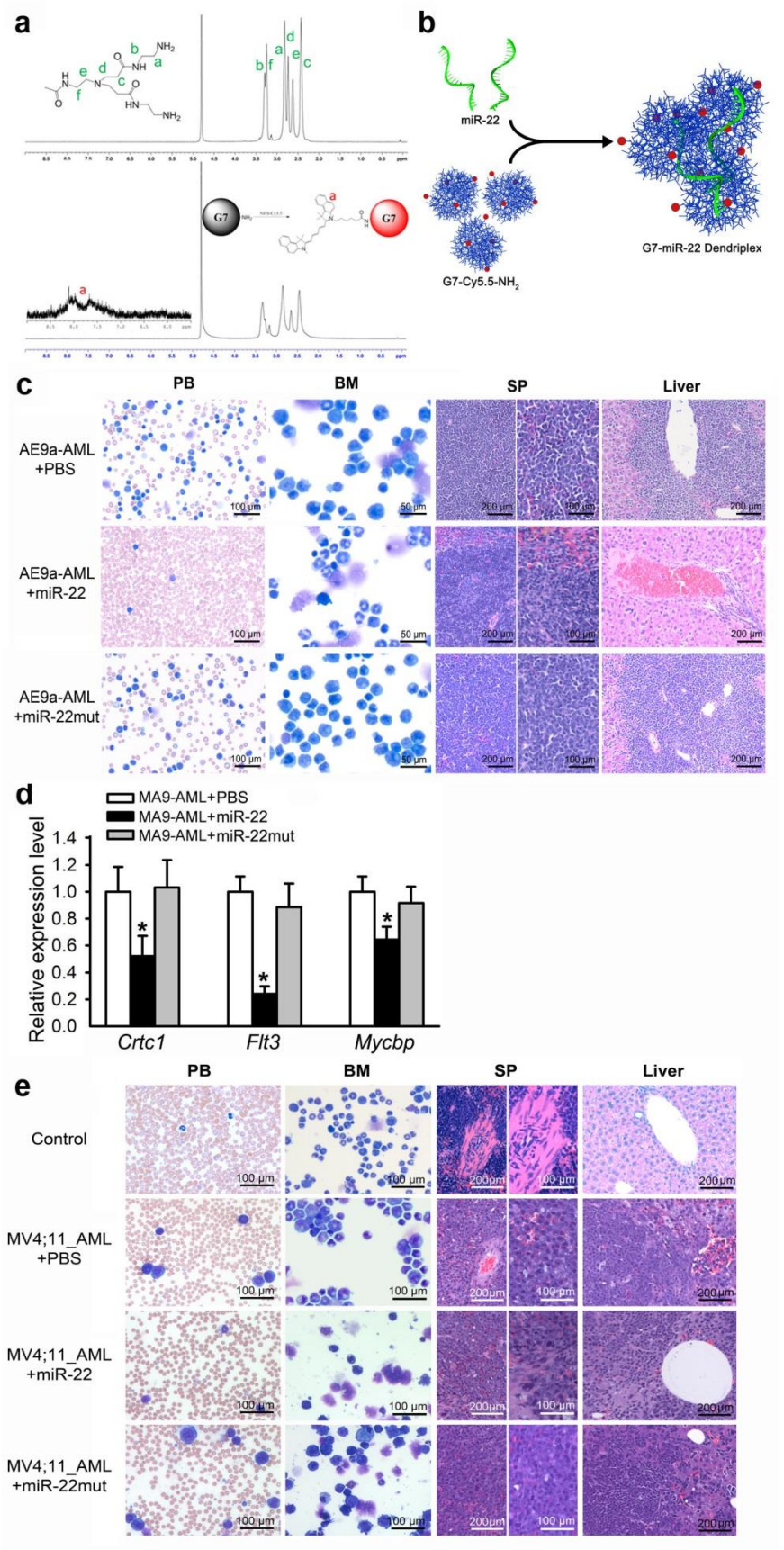
a
b
miR-22
G7-Cy5.5-NH2
G7-miR-22 Dendriplex
c
PB
BM
SP
Liver
AE9a-AML +PBS
AE9a-AML +miR-22
AE9a-AML +miR-22mut
d
MA9-AML+PBS
MA9-AML+miR-22
MA9-AML+miR-22mut
Relative expression level
Crtc1
Flt3
Mycbp
e
Control
MV4;11_AML +PBS
MV4;11_AML +miR-22
MV4;11_AML +miR-22mut

**Supplementary Figure 6.** The formation and effects of G7-Cy5.5-$NH_2$-miR-22 nanoparticles. (**a**) $^1$H NMR spectra of G7 PAMAM dendrimer (*upper panel*) and G7-Cy5.5-$NH_2$ (*lower panel*). Characteristic dendrimer peaks are located between 2.0–3.5 ppm. Following conjugation, there is an appearance of new peaks between 7.0-8.5 ppm due to the aromatic protons on Cy5.5, corresponding to approximately 4 Cy5.5 per G7. (**b**) Formation of the G7-miR-22 dendriplex. G7 PAMAM dendrimers were labeled using the near infrared dye, Cy5.5 (red dots), and mixed with miR-22. Complex formation is driven by electrostatic forces between the cationic primary amine surface groups of the PAMAM dendrimer and the anionic phosphate backbone of miR-22. Schematic represents approximate theoretical mixing ratio and sizes of polyplex components. (**c**) Wright-Giemsa stained PB and BM, and H&E stained spleen and liver of the *AE9a*-secondary leukemic mice treated with PBS control, miR-22 or miR-22 mutant nanoparticles. (**d**) Expression levels of *Crtc1, Flt3* and *Mycbp* in the BM cells of the PBS, miR-22- or miR-22 mutant-nanoparticle-treated secondary BMT recipient mice transplanted with *MLL-AF9* primary leukemic blast cells. Mean±SD values are shown. *, $p<0.05$, *t*-test. (**e**) Wright-Giemsa stained PB and BM, and H&E stained spleen and liver of the non-transplanted NSGS control or MV4;11 xenotransplanted NSGS leukemic mice treated with PBS control, miR-22 or miR-22 mutant nanoparticles.

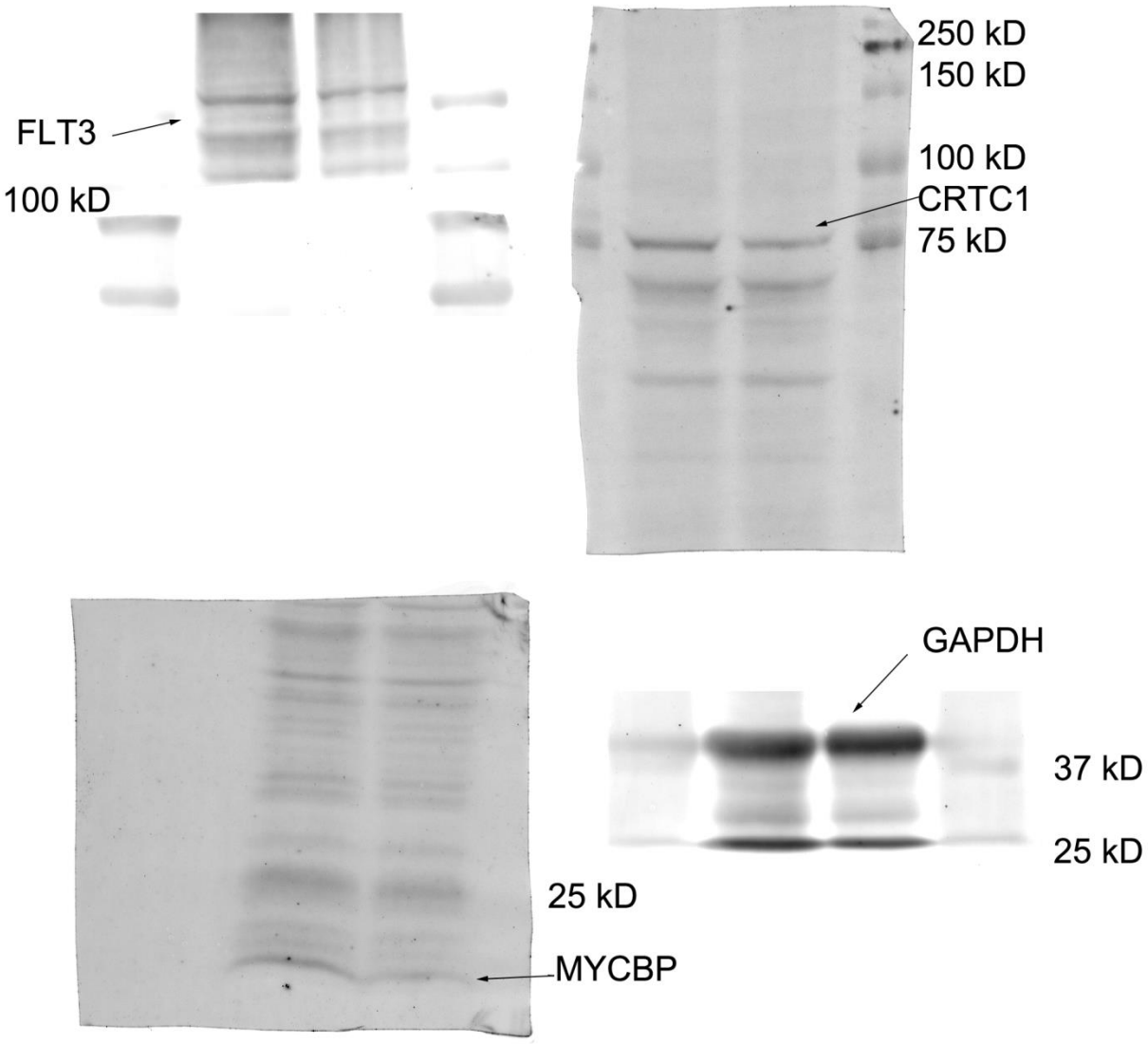


**Supplementary Figure 7. Original scans of Western blotting results shown as Supplementary Figure 3b.**

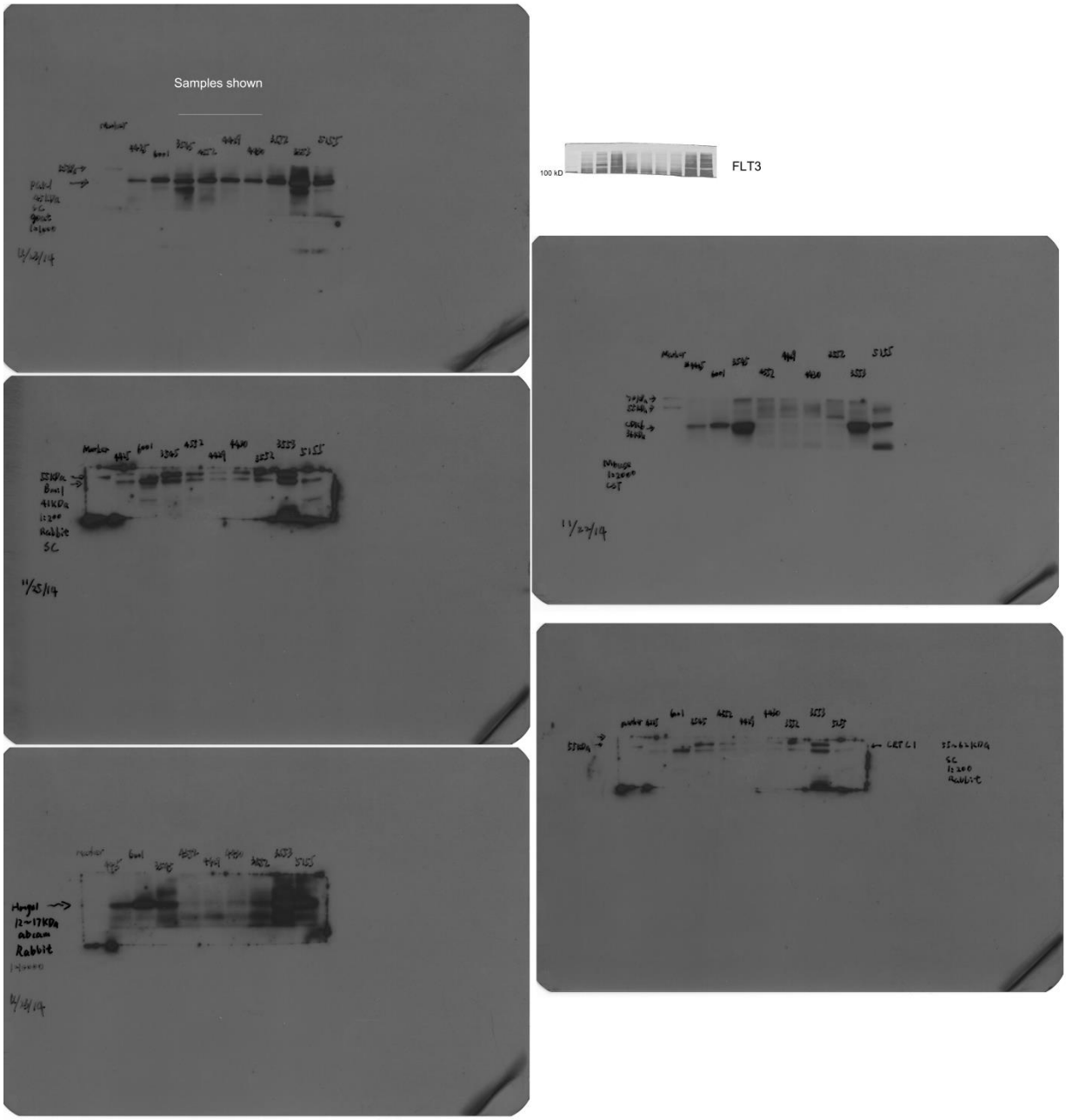


**Supplementary Figure 8. Original scans of Western blotting results shown as Supplementary Figure 3c.**

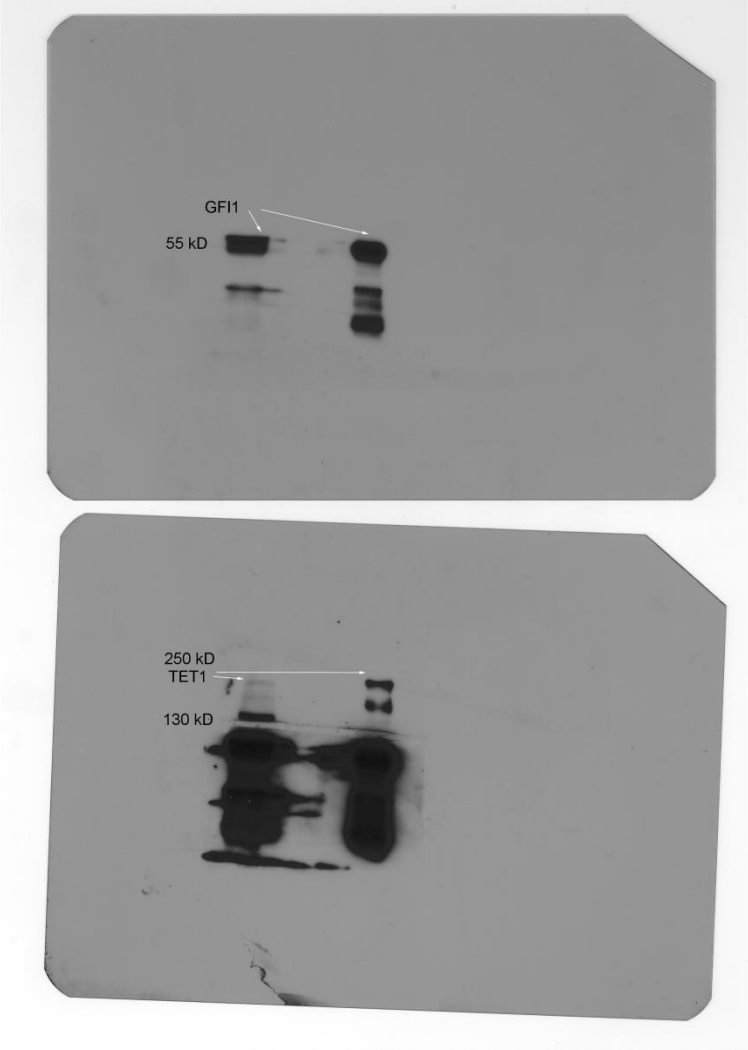


**Supplementary Figure 9. Original scans of Western blotting results shown as Figure 6c.**

**Supplementary Table 1. List of the 22 candidate target genes of miR-22 in AML**

| Gene | In-house_81S (Pearson correlation analysis of candidate targets and miR-22 in expression) | | TCGA_177S (Pearson correlation analysis of candidate targets and miR-22 in expression) | | 15-mouse-sample set (9 MLL-AF9 AML vs. 6 normal control samples; SAM) | | 109-human-sample set (100 AML vs. 9 normal control samples; SAM) | |
|---|---|---|---|---|---|---|---|---|
| | *r* | *p* | *r* | *p* | Fold change | *q*-value | Fold change | *q*-value |
| *ANKRD28* | -0.43 | 0.0001 | -0.34 | <0.0001 | 1.72 | <0.0001 | 1.67 | 0.0015 |
| *ANKRD52* | -0.22 | 0.0458 | -0.17 | 0.0199 | 1.22 | <0.0001 | 1.13 | 0.0348 |
| *B3GNTL1* | -0.41 | 0.0001 | -0.49 | <0.0001 | 1.28 | <0.0001 | 1.34 | 0.0107 |
| *CDK6* | -0.27 | 0.0139 | -0.34 | <0.0001 | 2.38 | <0.0001 | 1.15 | 0.0131 |
| *CRTC1* | -0.31 | 0.0045 | -0.16 | 0.0359 | 1.32 | <0.0001 | 1.18 | 0.0173 |
| *DDX51* | -0.36 | 0.0010 | -0.30 | 0.0001 | 1.65 | <0.0001 | 1.18 | 0.0112 |
| *DFFB* | -0.26 | 0.0185 | -0.19 | 0.0103 | 1.35 | <0.0001 | 1.19 | 0.0213 |
| *ETV6* | -0.31 | 0.0042 | -0.40 | <0.0001 | 1.70 | <0.0001 | 1.53 | 0.0044 |
| *FLT3* | -0.21 | 0.0307 | -0.35 | <0.0001 | 4.48 | <0.0001 | 2.12 | 0.0028 |
| *MBD3* | -0.28 | 0.0126 | -0.21 | 0.0048 | 1.31 | <0.0001 | 1.15 | 0.0238 |
| *METTL10* | -0.30 | 0.0066 | -0.20 | 0.0075 | 1.21 | 0.0053 | 1.32 | 0.0091 |
| *MFSD10* | -0.46 | <0.0001 | -0.28 | 0.0002 | 1.60 | <0.0001 | 1.61 | 0.0036 |
| *MTL5* | -0.29 | 0.0081 | -0.29 | 0.0001 | 1.50 | <0.0001 | 1.17 | 0.0407 |
| *MYCBP* | NA | NA | -0.15 | 0.0481 | 1.11 | 0.034 | NA | NA |
| *OLA1* | -0.31 | 0.0048 | -0.35 | <0.0001 | 1.37 | <0.0001 | 1.10 | 0.0446 |
| *RCC2* | -0.24 | 0.0323 | -0.23 | 0.0026 | 1.37 | 0.0002 | 1.33 | 0.0041 |
| *SGTA* | -0.34 | 0.0019 | -0.20 | 0.0082 | 1.13 | 0.0014 | 1.53 | <0.0001 |
| *SPATS2* | -0.33 | 0.0024 | -0.30 | 0.0001 | 1.05 | 0.052 | 1.21 | 0.0152 |
| *TRIM13* | -0.23 | 0.0392 | -0.31 | <0.0001 | 2.58 | <0.0001 | 1.46 | 0.0016 |
| *TRIM46* | -0.23 | 0.0387 | -0.26 | 0.0006 | 1.25 | <0.0001 | 1.27 | 0.0054 |

| | | | | | | | | |
|---|---|---|---|---|---|---|---|---|
| *ZCCHC3* | -0.26 | 0.0187 | -0.28 | 0.0001 | 1.63 | 0.0002 | 1.13 | 0.026 |
| *ZNF512B* | -0.39 | 0.0003 | -0.42 | <0.0001 | 2.03 | <0.0001 | 1.38 | 0.0019 |

Note: *r*, correlation coefficient; *p*, *p*-value; NA, not available. SAM, significant analysis of microarrays [1]. Notably, *MYCBP* was not included in Affymetrix GeneChip® Human Exon ST Arrays and thus it was absent in our in-house human AML datasets [2,3]; as a result, *MYCBP* was not shown in the original 21 candidate target gene list, although *MYCBP* exhibited a significant inverse correlation in expression with miR-22 in the TCGA dataset and was significantly up-regulated in the mouse AML dataset.

**Supplementary Table 2. List of functionally important downstream target genes of the CREB or MYC signaling pathways that exhibit a significant inverse correlation of expression with miR-22 in AML**

| **Signaling Pathway** | **Gene** | In-house_81S (Pearson correlation analysis of candidate genes and miR-22 in expression) | | TCGA_177S (Pearson correlation analysis of canddiate genes and miR-22 in expression) | |
|---|---|---|---|---|---|
| | | *r* | *p* | *r* | *p* |
| **CREB** | *CDK6* | -0.27 | 0.0139 | -0.34 | <0.0001 |
| | *HOXA7* | -0.29 | 0.0079 | -0.16 | 0.0345 |
| | *RGS2* | 0.39 | 0.0004 | 0.50 | <0.0001 |
| **MYC** | *BMI1* | -0.24 | 0.0335 | -0.12 | 0.0455 |
| | *FASN* | -0.29 | 0.0091 | -0.26 | 0.0004 |
| | *HMGA1* | -0.31 | 0.0051 | -0.18 | 0.0145 |

Note: *r*, correlation coefficient; *p*, *p*-value.

**Supplementary Table 3. Correlation between miR-22 and *TET1/2/3* or *GFI1* in expression in three AML patient cohorts***

| AML set | Gene | *r* | *p* |
|---|---|---|---|
| **In-house_81S (n=81)** | ***TET1*** | **-0.328** | 0.0014 |
| | ***TET2*** | **0.239** | 0.016 |
| | ***TET3*** | **0.013** | 0.45 |
| | ***GFI1*** | **-0.429** | <0.0001 |
| **TCGA_183S (n=183)** | ***TET1*** | **-0.380** | <0.0001 |
| | ***TET2*** | **0.356** | <0.0001 |
| | ***TET3*** | **0.327** | <0.0001 |
| | ***GFI1*** | **-0.249** | 0.0007 |
| **GSE37642_562S (n=562)** | ***TET1*** | **-0.395** | <0.0001 |
| | ***TET2*** | **0.140** | 0.0009 |
| | ***TET3*** | **0.294** | <0.0001 |
| | ***GFI1*** | **-0.262** | 0.0005 |

*Pearson Correlation analysis of *TET1/2/3* or *GFI1* with mature miR-22 (for In-house_81S) or precursor miR-22 (for TCGA_183S and GSE37642_562S) in expression was performed. *r*, correlation coefficient; *p*, *p*-value.

**Supplementary Table 4. Effects of G7-miR-22-nanoparticles on mouse blood cell differentiation.**

| | 4 W | | 8 W | | 12 W | | 16 W | | 20 W | | Normal range |
|---|---|---|---|---|---|---|---|---|---|---|---|
| | PBS | miR-22 | PBS | miR-22 | PBS | miR-22 | PBS | miR-22 | PBS | miR-22 | |
| **WBC (K/μl)** | 12.26 | 11.92 | 12.06 | 8.92 | 4.14 | 4.18 | 8.71 | 9.18 | 5.74 | 6.7 | 1.8-10.7 |
| **NE (K/μl)** | 2.79 | 2.04 | 2.33 | 1.85 | 0.57 | 0.06 | 1.16 | 0.61 | 0.68 | 0.88 | 0.1-2.4 |
| **LY (K/μl)** | 8.3 | 9.48 | 8.87 | 6.59 | 3.38 | 3.97 | 6.95 | 7.97 | 4.67 | 5.24 | 0.9-9.3 |
| **MO (K/μl)** | 0.43 | 0.3 | 0.5 | 0.46 | 0.12 | 0.14 | 0.36 | 0.29 | 0.33 | 0.44 | 0.0-0.4 |
| **EO (K/μl)** | 0.57 | 0.08 | 0.25 | 0.02 | 0.05 | 0 | 0.19 | 0.23 | 0.05 | 0.1 | 0.0-0.2 |
| **BA (K/μl)** | 0.16 | 0.01 | 0.11 | 0.01 | 0.01 | 0 | 0.06 | 0.09 | 0.01 | 0.03 | 0.0-0.2 |
| **RBC (M/μl)** | 11.68 | 10.74 | 12.2 | 10.57 | 9.41 | 11.78 | 11.51 | 12.35 | 7.71 | 9.41 | 6.36-9.42 |
| **PLT (K/μl)** | 728 | 875 | 847 | 1215 | 1253 | 1246 | 1007 | 1354 | 1070 | 873 | 592-2972 |

Note: Shown are data collected at the indicated time points (i.e. 4, 8, 12, 16 and 20 weeks) post single *i.v.* injection of 0.5 mg/kg of G7-miR-22-nanoparticles (miR-22) or PBS control (PBS). WBC = white blood cells; NE = neutrophils; LY = lymphocytes; MO = monocytes; EO = eosinophils; BA = basophils; RBC = red blood cells; PLT = platelets.

## SUPPLEMENTARY REFERENCES


1. Tusher, V.G., Tibshirani, R. & Chu, G. Significance analysis of microarrays applied to the ionizing radiation response. *Proc Natl Acad Sci USA* **98**, 5116-5121 (2001).
2. He, C., *et al.* Young intragenic miRNAs are less coexpressed with host genes than old ones: implications of miRNA-host gene coevolution. *Nucleic Acids Res* **40**, 4002-4012 (2012).
3. Huang, H., *et al.* TET1 plays an essential oncogenic role in MLL-rearranged leukemia. *Proc Natl Acad Sci U S A* **110**, 11994-11999 (2013).